Hindawi Publishing Corporation
Advances in Astronomy
Volume 2013, Article ID 746020, 8 pages
http://dx.doi.org/10.1155/2013/746020

Research Article

A Characterization of the Diffuse Galactic Emissions in the Anticenter of the Galaxy

L. Fauvet,[1,2] J. F. Macías-Pérez,[2] S. R. Hildebrandt,[2,3] and F.-X. Désert[4]

[1] *Astrophysics Division, Research and Scientific Support Department, European Space Agency (ESA), Keplerlaan 1, 2201 AZ Noordwijk, The Netherlands*

[2] *LPSC, Université Joseph Fourier Grenoble 1, CNRS/IN2P3, Institut National Polytechnique de Grenoble, 53 Avenue des Martyrs, 38026 Grenoble Cedex, France*

[3] *California Institute of Technology, 1200 E. California Boualevard, Pasadena, CA 91125, USA*

[4] *Laboratoire d'Astrophysique de Grenoble, IPAG, Université Joseph Fourier, BP 53, 38041 Grenoble Cedex 9, France*

Correspondence should be addressed to J. F. Macías-Pérez; macias@lpsc.in2p3.fr

Received 8 July 2012; Revised 27 November 2012; Accepted 20 December 2012

Academic Editor: Angelica de Oliveira-Costa

Using the Archeops and WMAP data, we perform a study of the anticenter Galactic diffuse emissions—thermal dust, synchrotron, free-free, and anomalous emissions—at degree scales. The high-frequency data are used to infer the thermal dust electromagnetic spectrum and spatial distribution allowing us to precisely subtract this component at lower frequencies. After subtraction of the thermal dust component, a mixture of standard synchrotron and free-free emissions does not account for the residuals at these low frequencies. Including the all-sky 408 MHz Haslam data we find evidence for anomalous emission with a spectral index of −2.5 in T_{RJ} units. However, we are not able to provide coclusion regarding the nature of this anomalous emission in this region. For this purpose, data between 408 MHz and 20 GHz covering the same sky region are needed.

1. Introduction

The anomalous microwave emission (AME in the following) is an important contributor of the Galactic diffuse emissions in the range from 20 to 60 GHz. It was first observed by [1, 2] and then identified by [3] as free-free emission from electrons with temperature $T_e > 10^6$ K. Draine and Lazarian [4] argued that AME may result from electric dipole radiation due to small rotating grains, the so-called *spinning dust*. Models of the *spinning dust* emission [5] show an electromagnetic spectra peaking at around 20–50 GHz being able to reproduce the observations [6–13]. The initial spinning dust model has been refined regarding the shape and rotational properties of the dust grains [14–17]. An alternative explanation of AME was proposed by Draine and Lazarian [18] based on magnetic dipole radiation arising from hot ferromagnetic grains. This kind of models associated to single domain predict polarization fraction much bigger than the electric dipole ones [19]. Original models have been mainly ruled out by many studies [10, 20–23] although modern variants of those may still be of interest (B. Draine private communication).

Correlation between microwave and infrared maps, mainly dominated by dust thermal emission [24], was observed for various experiments, for example, on COBE/DMR [2, 25], OVRO [3], Saskatoon [1], survey at 19 GHz [26], and Tenerife [27]. Similar signal was found in small region by [6] and in some molecular clouds based on data from COSMOSOMAS [8, 28], AMI (AMI Consortium [29, 30]), CBI [10, 31], VSA [13], and Planck [32]. Recent studies based on several sets of data [33] found similar results.

Independently, Bennett et al. [34] proposed an alternative explanation of AME based on flat-spectrum synchrotron emission associated to star-forming regions to explain part of the WMAP first-year observations. This hypothesis seems to be in disagreement with results from de Oliveira-Costa et al. [7]; Fernández-Cerezo et al. [35]; Hildebrandt et al. [36]; Ysard et al. [37], which showed that spinning dust was the most trustable emission to explain the excess below 20 GHz.

Furthermore, Davies et al. [38] showed the existence of important correlation between microwave and infrared emissions in regions outside star-forming areas. More recently, Kogut et al. [39] discussed the fact that *spinning dust* fits better to ARCADE data (3.8 and 10 GHz) than a flat-spectrum synchrotron.

We propose here to study the Galactic diffuse emissions in the Galactic plane, particularly focusing on the anticenter region. The observational data, from 408 MHz to 3000 GHz, used for this study are presented in Section 2. Section 3 discusses in details the contribution of the diffuse Galactic thermal dust emission using the high-frequency data. In Section 4, we consider a simple free-free and canonical synchrotron emission model for the thermal dust-subtracted microwave data. The possible contribution from anomalous emission is discussed in Section 5. We draw conclusions in Section 6.

2. Microwave and Millimeter Observations

We describe in this section the data used for the analysis presented in this paper. As we are interested in the Galactic diffuse emission, we consider only large coverage sky surveys in the radio, microwave, millimeter, and infrared domain including the 408 MHz all-sky survey and the WMAP ARCHEOPS and IRAS data.

2.1. The 408 MHz All-Sky Survey. In the radio domain, the 408 MHz all-sky continuum survey [40] at a resolution of 0.85 degrees is a good tracer of the synchrotron emission. In particular, we use the 408 MHz all-sky map available on the LAMBDA website in the HEALPix pixelisation scheme [41]. The 408 MHz all-sky survey map was smoothed down to a resolution of 1 degree and downgraded to $N_{\rm side} = 64$ in the HEALPix pixelisation scheme [41]. The uncertainties on this map are assumed to be of 10% following Haslam et al. [40] and are mainly due to calibration errors.

2.2. WMAP. In order to estimate the diffuse Galactic emission at microwave frequencies, we used the maps in temperature using the K, Ka, Q, V, and W band maps of the WMAP mission of its 7-years WMAP [42]. In particular, we used the coadded maps available on the the LAMBDA web site, also smoothed down to a resolution of 1 degree and downgraded to $N_{\rm side} = 64$. Uncertainties in the WMAP data were computed assuming an uncorrelated anisotropic noise as described in [42]. The variance per pixel at the working resolution was computed using the variance of a single hit and the number of hits per pixels.

2.3. Archeops. In the millimeter wavelengths, we use the ARCHEOPS balloon experiment [43] data. ARCHEOPS observed the sky at four frequency bands: 143, 217, 353, and 545 GHz, with resolutions of 11, 13, 12, and 18 arcmin respectively [44]. The ARCHEOPS survey covers about 30% of the sky mainly centered in the Galactic anti-center region. We use here the original ARCHEOPS maps which were also smoothed down to a resolution of one degree and downgraded to $N_{\rm side} = 64$.

2.4. IRAS. In the infrared, we have used the new generation of the IRAS data (*InfraRed Astronomical Satellite*) at 100 and 60 μm (3000 and 5000 GHz). This release of the IRAS data is called IRIS (*Improved Reprocessing of the* IRAS data) [45] and has been built with a better destriping ability, a better subtraction of the zodiacal light, and a calibration and a zero level compatible with the far infrared instrument, FIRAS, of COBE. The IRIS maps were also smoothed down to a resolution of one degree and downgraded to $N_{\rm side} = 64$.

In order to avoid the contamination from the CMB at intermediate frequencies, 30–200 GHz, we have restricted our study to the Galactic plane where the Galactic emissions dominate over the cosmological CMB emission. In practice, we selected those regions in the ARCHEOPS 353 GHz map with intensity above 3000 $\mu K_{\rm RJ}$ or higher. This corresponds to 1391 pixels at $N_{\rm side} = 64$ in the anticenter region.

3. Diffuse Galactic Thermal Dust Emission

We first study the electromagnetic and spatial properties of the thermal dust diffuse Galactic emission. In order to model the intensity of the thermal dust emission, we use a simple grey body spectrum of the form

$$I_\nu = I_0 \nu^{\beta_d} B_\nu (T_d), \tag{1}$$

where β_d is the spectral index of the thermal dust emission and T_d is the dust temperature.

We used the ARCHEOPS and IRIS 100 μm maps to characterize the dust thermal emission model. We fitted the data to the model pixel by pixel using as free parameters I_0, β_d, and T_d, and the following likelihood function

$$-\log \mathcal{L}_\nu = \sum_\nu \frac{\left(D_\nu^p - M_\nu^p\right)^2}{\sigma_\nu^{p\,2}}, \tag{2}$$

where D_ν^p and M_ν^p correspond to the data and model at the pixel p within the mask and for the observation frequency ν (=143, 217, 353, 545, and 3000 GHz). σ_ν^p is the $1-\sigma$ error bar associated with D_ν^p. β_d and T_d were explored using an uniformly spaced grid (as defined in Table 2), while I_0 was computed via a linear fit for each pair (β_d, T_d). The instrumental noise in the ARCHEOPS maps has been estimated using simulations of the noise in the ARCHEOPS Time Ordered Information (TOI) following the method described in Macías-Pérez et al. [44]. The variance per pixel was calculated from 250 simulated noise maps at one degree resolution and $N_{\rm side} = 64$. The error bars for the IRIS data at 100 μm were set to 13.5% following [45] as they are dominated by calibration errors.

In Figure 1 we, present maps of the dust temperature and spectral index within the considered mask. We also show the statistical uncertainties on these parameters. As expected,, the errors increase significantly on the edges of the

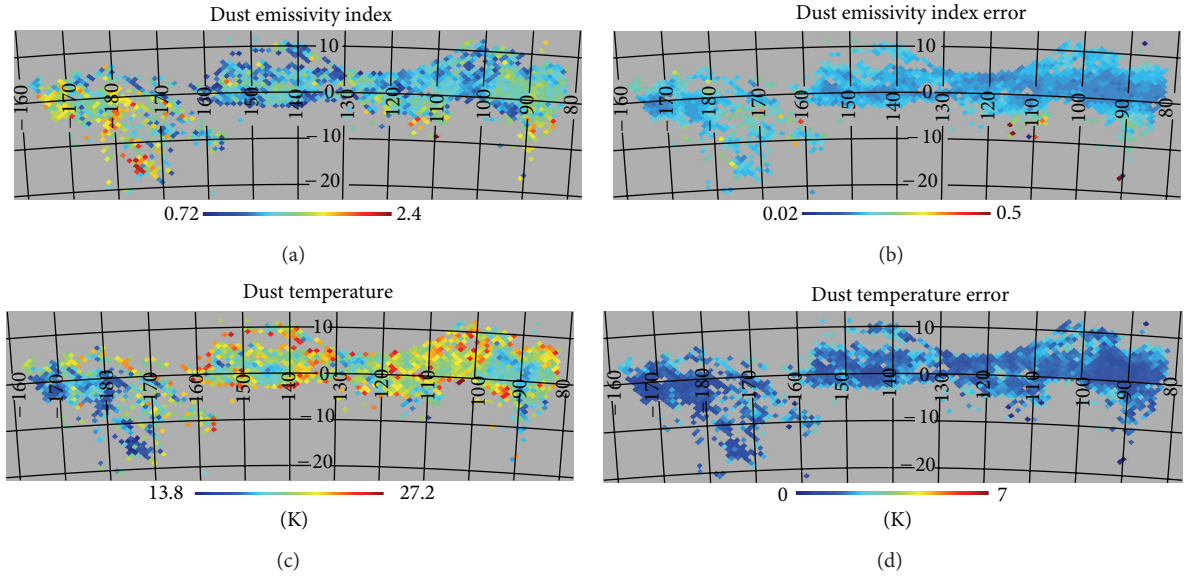

Figure 1: From top to bottom and from left to right: maps of the best-fit thermal dust emission spectral indices and temperature and uncertainties at 2σ (95% C.L.) (*right*).

maps. These noisy pixels will be excluded from the analysis hereafter. We can also notice that in the inner regions, the statistical errors are significantly smaller than the observed dispersion for the two parameters. We observe that the mean dust temperature is 20.0 K with 2.1 K dispersion, while the mean instrumental uncertainties are of the order of 1 K. In the same way, the mean dust spectral index is 1.40 with a dispersion of 0.25, and the mean instrumental uncertainties of the order of 0.1.

Figures 1 and 2 compare the best-fit thermal dust model to the IRAS and ARCHEOPS data. From left to right, we show the data, the model, and residuals for all frequencies. For the ARCHEOPS data, the residuals are at most 10% of the total intensity. In the case of the IRAS data, the model reproduce rather well the 100 μm map. However, at 60 μm, the residuals are important, and the model is not able reproduce the structure in the data. Residuals can be as important as 60% of the total intensity. This can be explained by the presence of a hotter dust component as discussed in Désert et al. [24]. This component is out of the scope of this study and does not have any consequence in the following study. Table 1 presents the rms of the ARCHEOPS and IRAS data as well as the rms of the residuals after subtraction of the dust model. The last column of the table represents the mean standard deviation of the noise in the original maps. We observe that except for the 5000 GHz data, the residuals are of the order of magnitude of the noise.

4. Diffuse Galactic Free-Free and Synchrotron Emissions

In order to estimate the contribution of the diffuse Galactic free-free emission, which is expected to be important at the WMAP bands, we use the *extinction-corrected h-alpha foreground template* (Hα) map built by Finkbeiner [6]. This map was computed using data from the *Virginia Tech Spectral line Survey* (VTSS) for the North and of data from the *Southern H-Alpha Sky Survey Atlas* (SHASSA) for the South sky (Figure 3). Correction factors are applied to take into account dust absorption [6]. We started from a map at resolution $N_{\rm side} = 512$ and downgraded it, as the other maps, at a resolution of $N_{\rm side} = 64$. In order to obtain a template of the free-free emission at 23 GHz using the Hα map, we follow Bennett et al. [34]. In antenna temperature units and defining the emission measure as $\mathrm{EM} = \int n_e^2 dn$, one can write

$$T_A^{\rm ff}(\mu\mathrm{K}) = 1.44\,\mathrm{EM}_{\mathrm{cm}^{-6}\cdot\mathrm{pc}} \cdot \frac{\left[1+0.22\ln\left(T_e/8000\,\mathrm{K}\right)-0.14\ln\left(\nu/41\mathrm{GHz}\right)\right]}{\left(\nu/41\mathrm{GHz}\right)^2\left(T_e/8000\,\mathrm{K}\right)^{1/2}}. \quad (3)$$

The intensity of the Hα $I(R)$ emission (in Rayleigh units) is defined by

$$I(R) = 0.44\,\mathrm{EM}_{\mathrm{cm}^{-6}\cdot\mathrm{pc}}\left(\frac{T_e}{8000\,\mathrm{K}}\right)^{-1/2} \times\left(1-0.34\ln\left(\frac{T_e}{8000\,\mathrm{K}}\right)\right). \quad (4)$$

Thus, the intensity of the free-free emission (in $\mathrm{mK_{RJ}}$) is given as a function of the intensity of the Hα emission (in Rayleighs) by

$$T_{\rm ff} = \frac{1.44}{0.44} I(R) \times \frac{\left(1+0.22\ln\left(T_e/8000\,\mathrm{K}\right)-0.14\ln\left(\nu/41\,\mathrm{GHz}\right)\right)}{\left(\nu/41\,\mathrm{GHz}\right)^2\left(1-0.34\ln\left(T_e/8000\,\mathrm{K}\right)\right)}. \quad (5)$$

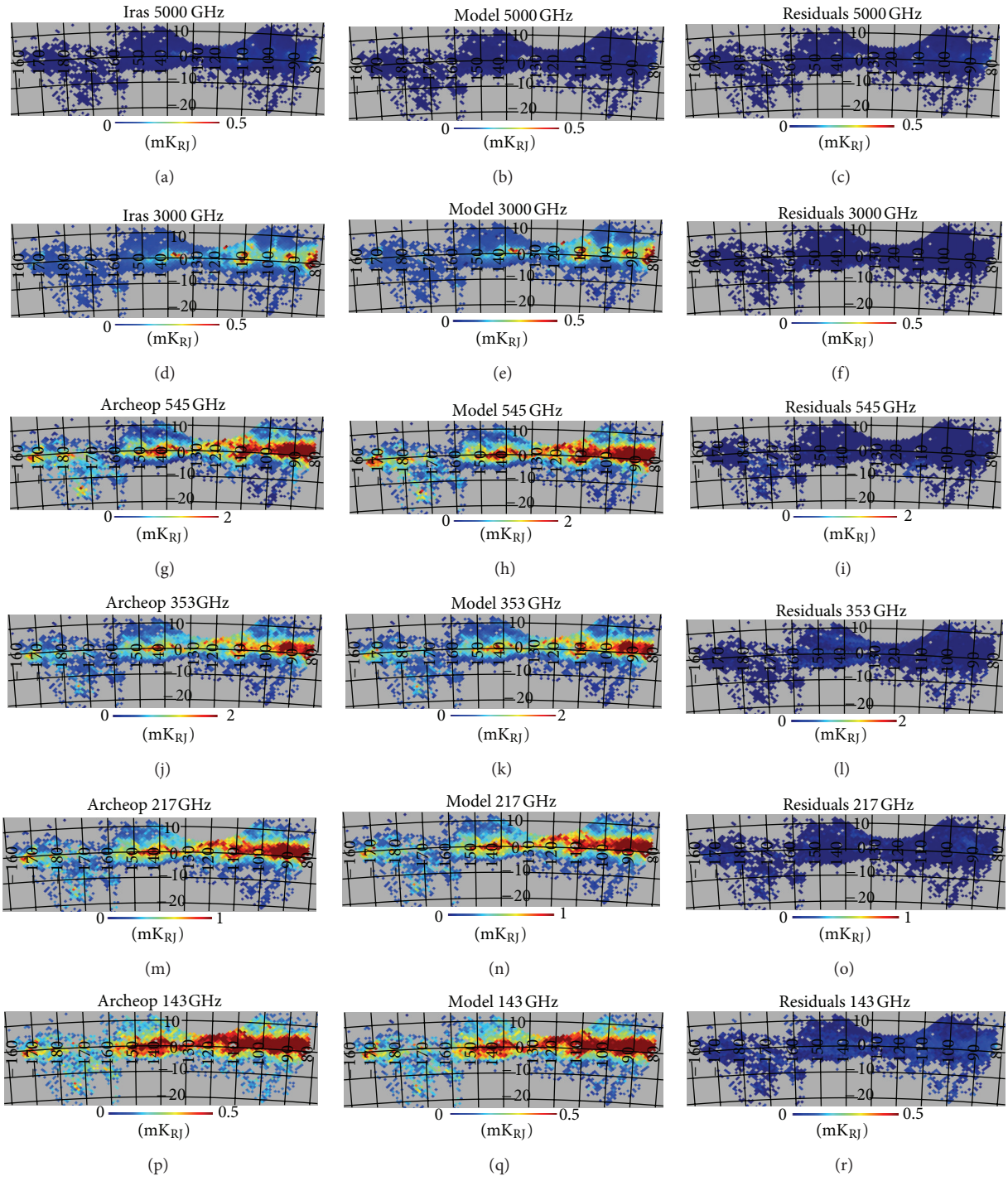

FIGURE 2: Temperature maps (mK$_{RJ}$) for the ARCHEOPS data (*left*), the thermal dust emission model (*center*), and residuals (*right*). From top to bottom, we present the 545, 353, 217, and 143 GHz maps.

We have extrapolated this free-free emission template at each of the WMAP frequencies assuming that the electromagnetic spectrum of the free-free emission is well represented by a power law of the form $\nu^{\beta_{\mathrm{ff}}}$ [34], where

$$\beta_{\mathrm{ff}} = -2 - \frac{1}{10.48 + 1.5 \ln\left(T_e/8000\,\mathrm{K}\right) - \ln\left(\nu/41\,\mathrm{GHz}\right)}. \quad (6)$$

We set a standard value for the electronic temperature at 8000 K, following [46]. The values of the spectral index obtained at the WMAP frequencies assuming these hypotheses are given in Table 3.

In order to model the synchrotron contribution, we used the 408 MHz *all-sky continuum survey* as a template map. We extrapolated it at all the considered frequencies assuming a power law-like electromagnetic spectrum in

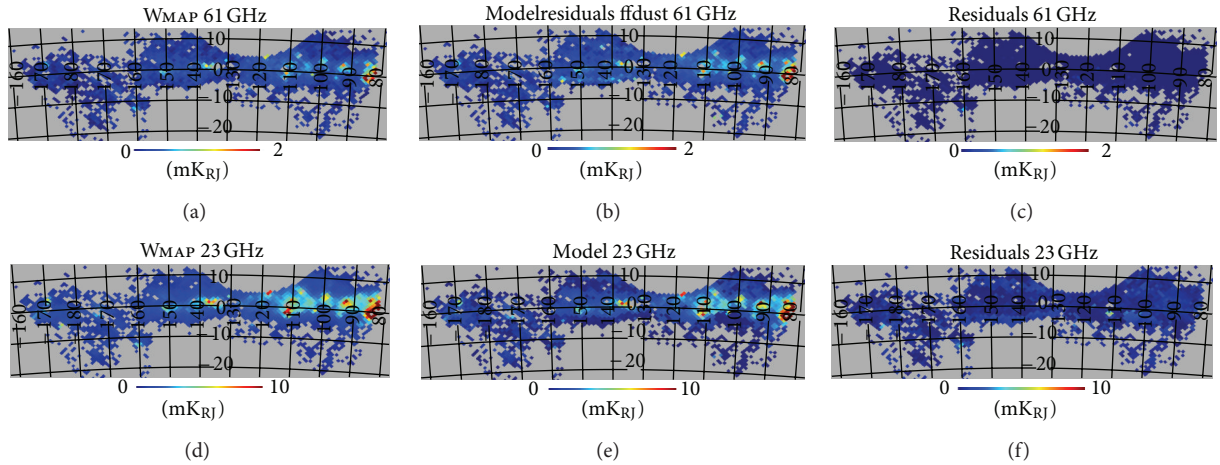

FIGURE 3: From left to right: residuals after subtraction of the thermal dust and free-free and anomalous emission models for the 61 (top) and 23 GHz (bottom) maps.

TABLE 1: Rms of the high-frequency data and of the residuals after subtraction of the dust model.

Frequency (GHz)	Data rms (mK$_{RJ}$)	Residual rms (mK$_{RJ}$)	Noise standard deviation (mK$_{RJ}$)
143	0.194407	0.0240274	0.0241575
217	0.315175	0.0306455	0.0406982
353	0.498923	0.0705655	0.0404479
545	0.699145	0.113738	0.157994
3000	0.0973817	0.00830546	0.0197808
5000	0.0134645	0.00974734	0.00176314

TABLE 2: Range of values considered for the parameters of the thermal dust emissivity model.

Parameters	Range	Step
β_d	[−1.0, 4.0]	0.02
T_d	[10.0, 37.0]	0.1

TABLE 3: Spectral index of the free-free emission at the WMAP frequencies assuming an electronic temperature of $T_e = 8000$ K.

Central frequency (GHz)	23	33	41	61	94
β_{ff}	−2.090	−2.093	−2.095	−2.099	−2.103

TABLE 4: Range of the parameters considered for the anomalous and free-free emission models.

Parameters	Ranges	Step
β_s	[−3.7, −2.3]	0.01
T_e (K)	[4000.0, 14000]	1000

antenna temperature with fix spectral index that we set to −2.7 [34].

In the second column of Table 5, we present the rms of the residuals after subtraction, of the Galactic thermal dust, synchrotron and free-free emission models. These residuals are significant: up to 90% of the original emission (first column of the table). We have observed both point-like and diffuse structures in these residuals. The former are more probably related to uncertainties in the modeling of the free-free emission. By contrast, the extra diffuse emission is most probably related to anomalous emission. This hypothesis is considered in the following section.

5. Study of the Anomalous Emission

In the previous section, we concluded that the observed emission in the range from 23 to 94 GHz cannot be explained only by the combination of the canonical Galactic diffuse emission: thermal dust, soft synchrotron, and free-free emission. Indeed, we have observed that in some compact regions there seems to be extra free-free emission with respect to the predictions from the Hα template. Furthermore, the diffuse emission is underestimated in general indicating either an extra component or a softer synchrotron component. In order to investigate these two problems, we have considered a two-component model composed of free-free and anomalous emissions in addition to diffuse thermal dust emission. We assume that the free-free and the anomalous emissions follow a simple power-law model such that

$$M_\nu = A_{\text{anom}}\nu^{\beta_{\text{anom}}} + A_{\text{ff}}\nu^{\beta_{\text{ff}}(T_e,\nu)}, \quad (7)$$

where M_ν are the observed maps in K$_{RJ}$ units at the frequency ν after subtraction of the contribution from thermal dust. Finally, we consider 4 free parameters in the model: the

Table 5: Rms of the WMAP data and of the residuals after subtraction of the dust, free-free, and standard synchrotron model and of the dust, free-free, and anomalous emission model compared to the standard deviation of the noise.

Frequency (GHz)	Data rms (mK_{RJ})	Residual DFS rms (mK_{RJ})	Residual DFA rms (mK_{RJ})	Noise standard deviation (mK_{RJ})
23	2.03831	2.02387	0.353262	0.183557
33	0.907433	0.884012	0.0881647	0.0612279
41	0.562764	0.531677	0.0372230	0.0438113
61	0.256907	0.205086	0.0377750	0.0205909
94	0.209367	0.112932	0.0530679	0.0239733

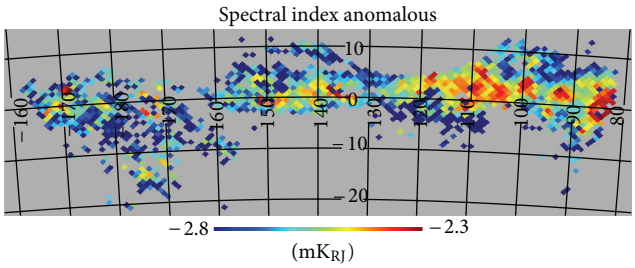

Figure 4: Map of the spectral index of the anomalous emission (*right*).

normalization coefficients $A_{\rm sync}$ and $A_{\rm ff}$, the spectral index β_s of the anomalous component, and the free electron temperature. To simplify the fitting procedures, we vary β_s and T_e in the ranges shown in Table 4. Notice that we have not explicitly considered the canonical synchrotron emission in this model. Indeed, our so-called anomalous component will be a mixture of real anomalous emission and canonical synchrotron emission.

We fit this two-component model to the dust-subtracted WMAP maps and to the 408 MHz map for which the thermal dust emission is negligible. As discussed before, the uncertainties on the WMAP data have been calculated assuming anisotropic white noise on the maps. We compute the variance r pixel using the variance per single observation provided on the LAMBDA website and maps of the number of hit counts. For the 408 MHz map, we assume 10% uncertainties as discussed in Section 2. It is important to notice that an alternative three-component model (including free-free, canonical synchrotron, and anomalous emissions) would imply at least 6 free parameters to be fitted on only 6 sky maps. That is why we have chosen to consider a two-component model only.

From the results of the fit, we observe that the anomalous emission seems to dominate the diffuse component at 1 GHz, while the free-free emission seems to be mainly located in few compact regions. In Figure 4, we present the map of the reconstructed spectral index for the anomalous emission, β_s. We observe that the anomalous emission seems to be well represented by a power law with average spectra index of −2.5. Similar results have been found by Bennett et al. [34] and Hinshaw et al. [47] who claim conclusive evidence for hard synchrotron emission. In our analysis, we did not dispose of data in the frequency range from 10 to 20 GHz to discriminate between this hypothesis and spinning dust emission (refer to [4] for a more complete review on spinning dust emission). It is important to notice that, currently, spinning dust emission has mainly been found in particular Galactic clouds (e.g., see [8, 27, 32, 33, 36, 37, 48–50]). Regarding the electron temperature, we have found that a physically accessible temperature is associated to only 40 out of 1039 pixels considered. These pixels correspond to the intense regions on the free-free map at 1 GHz. For the other pixels, the temperature is higher than the upper limit allowed [46] and then can not be linked to the free-free emission.

6. Summary and Conclusions

We have presented in this paper a detailed analysis of the Galactic diffuse emissions at the Galactic anticenter in the frequency range from 23 to 545 GHz. We have shown that a simple grey-body model can be used to describe the thermal dust emission in the frequency range from 100 to 3000 GHz. We find a mean temperature of 20 K with an intrinsic dispersion of 2.1 K and a spectral index of 1.4 with intrinsic dispersion of 0.25. These values are significantly larger and lower than expected from canonical models of the dust emission, $T_{\rm dust} \sim 17$ K and $\beta_{\rm dust} = 1.8$–2 (e.g., see [51, 52]). The same kind of results have been found by Ade et al. [53] although as they fixed the spectral index to 1.8, they obtains a lower temperature of 14 K. We have performed a similar analysis fixing $\beta_{\rm dust} = 1.8$, and we have also obtained lower dust temperatures. At high frequencies (above 3000 GHz), extra hot thermal dust emission from small dust grains is needed to account for the observations [24].

The former dust models have been used to extrapolate the thermal dust emission to microwave frequencies from 23 to 100 GHz. After subtraction of the thermal dust emission, we have shown that the microwave data can not be simply explained by a combination of free-free and canonical synchrotron emission. A more detailed analysis including AME has shown that the latter can be well approximated by a power law of average spectral index −2.5 in K_{RJ} units. This anomalous emission seems to dominate the diffuse emission at microwave frequencies, while free-free emission seems to be located in few compact regions. Indeed, we have found that outside those regions, the data that required electron temperature has not been physically meaningful.

The spectral index found for the anomalous emission is consistent with hard synchrotron emission [34, 47]. However, we can not formally conclude on this as our analysis did not include data in the 1 to 20 GHz that would help discriminating

this hypothesis from spinning dust emission by Draine and Lazarian [4] for which conclusive evidence has been found on some Galactic clouds by de Oliveira-Costa et al. [27, 48]; Lagache [49]; Watson et al. [8]; Ysard et al. [37]; Dickinson et al. [50]; Bot et al. [33]; Ade et al. [32], and as diffuse emission by Hildebrandt et al. [36].

Acknowledgments

The authors would like to thank R. Davies and C. Dickinson for useful discussions. S. R. Hildebrandt would like to thank the LPSC and, especially, Dr. Juan Macias and Professor Daniel Santos for the time they spent at LPSC during 2010.

References

[1] A. de Oliveira-Costa, A. Kogut, M. J. Devlin, C. B. Netterfield, L. A. Page, and E. J. Wollack, "Galactic microwave emission at degree angular scales," *The Astrophysical Journal Letters*, vol. 482, no. 1, pp. L17–L20, 1997.

[2] A. Kogut, A. J. Banday, and C. L. Bennett, "High-latitude Galactic emission in the cobe differential microwave radiometer 2 year sky maps," *The Astrophysical Journal*, vol. 460, p. 1, 1996.

[3] E. M. Leitch, A. C. S. Readhead, T. J. Pearson, and S. T. Myers, "An anomalous component of Galactic emission," *The Astrophysical Journal Letters*, vol. 486, no. 1, pp. L23–L26, 1997.

[4] B. Draine and A. Lazarian, "Diffuse Galactic emission from spinning dust grains," *The Astrophysical Journal Letters*, vol. 494, no. 1, pp. L19–L22, 1998.

[5] B. Draine and A. Lazarian, "Electric dipole radiation from spinning dust grains," *The Astrophysical Journal*, vol. 508, no. 1, p. 57, 1998.

[6] D. P. Finkbeiner, "A full-sky Hα template for microwave foreground prediction," *The Astrophysical Journal Supplement Series*, vol. 146, no. 2, pp. 407–415, 2003.

[7] A. de Oliveira-Costa, M. Tegmark, R. D. Davies et al., "The quest for microwave foreground X," *The Astrophysical Journal*, vol. 606, no. 2, pp. L89–L92, 2004.

[8] R. Watson, R. Rebolo, J. A. Rubino-Martin et al., "Detection of anomalous microwave emission in the Perseus molecular cloud with the COSMOSOMAS experiment," *The Astrophysical Journal Letters*, vol. 624, no. 2, pp. L89–L92, 2005.

[9] S. Iglesias-Groth, "Electric dipole emission by fulleranes and Galactic anomalous microwave emission," *The Astrophysical Journal Letters*, vol. 632, no. 1, p. 25, 2005.

[10] S. Casassus, G. F. Cabrera, F. Förster, T. J. Pearson, A. C. S. Readhead, and C. Dickinson, "Morphological analysis of the centimeter-wave continuum in the dark cloud LDN 1622," *The Astrophysical Journal*, vol. 639, pp. 951–964, 2006.

[11] S. Casassus, C. Dickinson, K. Cleary et al., "Centimetre-wave continuum radiation from the ρ Ophiuchi molecular cloud," *Monthly Notices of the Royal Astronomical Society*, vol. 391, no. 3, pp. 1075–1090, 2008.

[12] C. Dickinson, R. D. Davies, and J. R. Allison, "Anomalous microwave emission from the HII region RCW175," *The Astrophysical Journal*, vol. 690, no. 2, pp. 1585–1589, 2009.

[13] C. T. Tibbs, R. A. Watson, and C. Dickinson, "Very Small Array observations of the anomalous microwave emission in the Perseus region," *Monthly Notices of the Royal Astronomical Society*, vol. 402, no. 3, pp. 1969–1979, 2010.

[14] Y. Ali-Haïmoud, C. M. Hirata, and C. Dickinson, "A refined model for spinning dust radiation," *Monthly Notices of the Royal Astronomical Society*, vol. 395, no. 2, pp. 1055–1078, 2009.

[15] T. Hoang, B. T. Draine, and A. Lazarian, "Improving the model of emission from spinning dust: effects of grain wobbling and transient spin-up," *The Astrophysical Journal Letters*, vol. 715, no. 2, pp. 1462–1485, 2010.

[16] T. Hoang, A. Lazarian, and B. T. Draine, "Spinning dust emission: effects of irregular grain shape, transient heating, and comparison with *Wilkinson Microwave Anisotropy Probe* results," *The Astrophysical Journal*, vol. 741, no. 2, p. 87, 2011.

[17] K. Silsbee, Y. Ali-Haïmoud, and C. M. Hirata, "Spinning dust emission: the effect of rotation around a non-principal axis," *Monthly Notices of the Royal Astronomical Society*, vol. 411, pp. 2750–2769, 2011.

[18] B. T. Draine and A. Lazarian, "Magnetic dipole microwave emission from dust grains," *The Astrophysical Journal Letters*, vol. 512, no. 2, pp. 740–754, 1999.

[19] A. Lazarian and B. T. Draine, "Resonance paramagnetic relaxation and alignmentof amall grains," *The Astrophysical Journal*, vol. 536, no. 1, pp. L15–L18, 2000.

[20] E. S. Battistelli, R. Rebolo, and J. R. Martín, "Polarization observations of the anomalous microwave emission in the Perseus molecular complex with the cosmosomas experiment," *The Astrophysical Journal*, vol. 645, no. 2, pp. L141–L144, 2006.

[21] A. Kogut, "Three-year *Wilkinson Microwave Anisotropy Probe (WMAP)* observations: foreground polarization," *The Astrophysical Journal*, vol. 665, no. 1, pp. 335–362, 2007.

[22] B. S. Mason, T. Robishaw, C. Heiles, D. Finkbeiner, and C. Dickinson, "A limit on the polarized anomalous microwave emission of lynds 1622," *The Astrophysical Journal Letters*, vol. 697, no. 2, pp. 1187–1193, 2009.

[23] C. Lòpez-Caraballo, J. R. Martín, R. Rebolo, and R. Génova-Santos, "Constraints on the polarization of the anomalous microwave emission in the Perseus molecular complex from 7-year *WMAP* data," *The Astrophysical Journal*, vol. 729, no. 1, p. 25, 2011.

[24] F. X. Désert, F. Boulanger, and J. Puget, "Interstellar dust models for extinction and emission," *Astronomy and Astrophysics*, vol. 237, no. 1, pp. 215–236, 1990.

[25] A. Kogut, A. J. Banday, and C. L. Bennett, "Microwave emission at high Galactic latitudes in the four-year DMR sky maps," *The Astrophysical Journal Letters*, vol. 464, no. 1, p. L5, 1996.

[26] A. de Olivera-Costa, M. Tegmark, L. A. Page, and S. P. Boughn, "Galactic emission at 19 GHz," *The Astrophysical Journal Letters*, vol. 509, no. 1, pp. L9–L12, 1998.

[27] A. de Oliveira-Costa, M. Tegmark, C. M. Gutierrez et al., "Cross-correlation of tenerife data with Galactic templates-evidence for spinning dust?" *The Astrophysical Journal Letters*, vol. 527, no. 1, pp. L9–L12, 1999.

[28] R. Génova-Santos, R. Rebolo, J. R. Martín, C. H. C. Lòpez-Caraballo, and S. Hildebrandt, "Detection of anomalous microwave emission in the *Pleiades Reflection Nebula with WMAP* and the COSMOSOMAS experiment," *The Astrophysical Journal*, vol. 743, no. 1, p. 67, 2011.

[29] A. M. M. Scaife, N. Hurley-Walker, D. A. Green et al., "An excess of emission in the dark cloud LDN1111 with the Arcminute Microkelvin Imager," *Monthly Notices of the Royal Astronomical Society*, vol. 394, no. 1, pp. L46–L50, 2009.

[30] A. M. M. Scaife, N. Hurley-Walker, D. A. Green et al., "AMI observations of Lynds dark nebulae: further evidence for

anomalous cm-wave emission," *Monthly Notices of the Royal Astronomical Society*, vol. 400, no. 3, pp. 1394–1412, 2009.

[31] P. Castellanos, S. Casassus, S. Dickinson et al., "Dust-correlated centimetre-wave radiation from the M78 reflection nebula," *Monthly Notices of the Royal Astronomical Society*, vol. 411, no. 2, pp. 1137–1150, 2011.

[32] Planck-Collaboration, "*Planck* early results. XX. New light on anomalous microwave emission from spinning dust grains," *Astronomy and Astrophysics*, vol. 536, article A20, 17 pages, 2011.

[33] C. Bot, N. Ysard, D. Paradis et al., "Submillimeter to centimeter excess emission from the Magellanic Clouds II. On the nature of the excess," *Astronomy and Astrophysics*, vol. 532, article A20, 7 pages, 2010.

[34] C. Bennett, M. Halpern, G. Hinshaw et al., "First-year *Wilkinson Microwave Anisotropy Probe* (*WMAP*) observations: preliminary maps and basic results ," *The Astrophysical Journal Supplement Series*, vol. 148, no. 1, article 1, 2003.

[35] S. Fernández-Cerezo, C. M. Gutièrrez, and R. Rebolo, "Observations of the cosmic microwave background and Galactic foregrounds at 12–17 GHz with the COSMOSOMAS experiment," *Monthly Notices of the Royal Astronomical Society*, vol. 370, no. 1, pp. 15–24, 2006.

[36] S. Hildebrandt, R. Rebolo, J. A. Rubino-Martín et al., "COSMOSOMAS observations of the cosmic microwave background and Galactic foregrounds at 11 GHz: evidence for anomalous microwave emission at high Galactic latitude," *Monthly Notices of the Royal Astronomical Society*, vol. 382, no. 2, pp. 594–608, 2007.

[37] N. Ysard, M. A. Miville-Deschênes, and L. Verstraete, "Probing the origin of the microwave anomalous foreground," *Astronomy and Astrophysics*, vol. 509, article 1, 4 pages, 2010.

[38] R. D. Davies, C. Dickinson, A. J. Banday, T. R. Jaffe, K. M. Górski, and R. J. Davis, "A determination of the spectra of Galactic components observed by the *Wilkinson Microwave Anisotropy Probe*," *Monthly Notices of the Royal Astronomical Society*, vol. 370, no. 3, pp. 1125–1139, 2006.

[39] A. Kogut, D. J. Fixsen, and S. M. Levin, "ARCADE 2 observations of Galactic radio emission," *The Astrophysical Journal*, vol. 734, no. 1, p. 4, 2011.

[40] C. Haslam, C. Salter, H. Stoffel, and W. E. Wilson, "A 408 MHz All-sky continuum survey II—the atlas of contour maps," *Astronomy and Astrophysics Supplement Series*, vol. 47, pp. 1–143, 1982.

[41] K. Gòrski, E. Hivon, A. Banday et al., "HEALPix: a framework for high-resolution discretization and fast analysis of data distributed on the sphere," *The Astrophysical Journal*, vol. 622, no. 2, pp. 759–771, 2005.

[42] G. Hinshaw, M. Nolta, C. Bennett et al., "Five-year *Wilkinson Microwave. Anisotropy Probe (WMAP)* observations: data processing, sky maps, and basic results," *The Astrophysical Journal Supplement Series*, vol. 180, no. 2, p. 225, 2009.

[43] A. Benoît, P. Ade, A. Amblard et al., "First detection of polarization of the submillimetre diffuse Galactic dust emission by Archeops," *Astronomy and Astrophysics*, vol. 424, pp. 571–582, 2004.

[44] J. Macías-Pérez, G. Lagache, B. Maffei et al., "Archeops in-flight performance, data processing, and map making," *Astronomy and Astrophysics*, vol. 467, no. 3, pp. 1313–1344, 2007.

[45] M. A. Miville-Deschênes and G. Lagache, "IRIS: a new generation of *IRAS* maps," *The Astrophysical Journal Supplement Series*, vol. 157, no. 2, pp. 302–323, 2005.

[46] B. Otte, J. Gallagher, and R. J. Reynolds, "Emission-line ratios and variations in temperature and ionization state in the diffuse ionized gas of five edge-on galaxies," *The Astrophysical Journal*, vol. 572, no. 2, p. 823, 2002.

[47] G. Hinshaw, M. R. Nolta, C. L. Bennett et al., "Three-year *Wilkinson Microwave Anisotropy Probe* (*WMAP*) observations: temperature analysis," *The Astrophysical Journal Supplement Series*, vol. 170, no. 2, p. 288, 2007.

[48] A. de Oliveira-Costa, M. Tegmark, D. P. Finkbeiner et al., "A new spin on Galactic dust," *The Astrophysical Journal Letters*, vol. 567, no. 1 I, pp. 363–369, 2002.

[49] G. Lagache, "The large-scale anomalous microwave emission revisited by *WMAP*," *Astronomy and Astrophysics*, vol. 405, no. 3, pp. 813–819, 2003.

[50] C. Dickinson, S. Casassus, R. Davies et al., "Infrared-correlated 31-GHz radio emission from Orion East," *Monthly Notices of the Royal Astronomical Society*, vol. 407, no. 4, pp. 2223–2229, 2010.

[51] D. P. Finkbeiner, M. Davis, and D. J. Schlegel, "Extrapolation of Galactic dust emission at 100 microns to cosmic microwave background radiation frequencies using FIRAS," *The Astrophysical Journal Letters*, vol. 524, no. 2, pp. 867–886, 1999.

[52] P. A. R. Ade, N. Aghanim, M. Arnaud et al., "*Planck*early results. XXIV. Dust in the diffuse interstellar medium and the Galactic halo," *Astronomy and Astrophysics*, vol. 536, article A24, 30 pages, 2011.

[53] P. A. R. Ade, N. Aghanim, M. Arnaud et al., "*Planck* early results: all sky temperature and dust optical depth from *Planck* and IRAS: constraints on the "dark gas" in our galaxy," *Astronomy and Astrophysics*, vol. 536, article A19, 16 pages, 2011.